FLICKER NOISE IN HARMONIC REJECTING CURRENT COMMUTATING PASSIVE FET MIXERS

Ludwig Lubich

Technical University of Sofia, Faulty of Telecommunications
1000 Sofia, 8 Kl. Ohridski Blvd
lvl@tu-sofia.bg

Abstract

The paper examines the flicker noise contribution of different FETs in harmonic rejection mixers (HRM) to the total mixer noise, using simple physical models. There are several different mechanisms which transfer the FETs' flicker noise to the mixer output. Equations for the level of flicker noise due to each noise transfer mechanism have been derived. Comparison between HRM and ordinary double balanced mixers in terms of flicker noise level has been made.

1. INTRODUCTION

Harmonics in the waveform of the local oscillator (LO) make the heterodyne receivers susceptible to interference from signals with frequencies $f = nf_{LO} \pm f_i$, where f_i is the intermediate frequency (IF) used. Traditionally high-order preselect filters are used to solve this problem. However, they are difficult or impossible to integrate on-chip.

In the recent years, harmonic rejection mixers (HRM) have gained in popularity as they allow to considerably relax the requirements on the receivers' preselect filters.

An HRM consists of several parallel operating elementary mixers, driven by multiphase LO. Their output signals, multiplied by different weighting factors, are summed. An HRM is equivalent to a single mixer, driven by an effective LO waveform from which some harmonics are excluded [1]. Usually, the effective LO waveform is based on a sampled sinusoid with N samples per period. Then the effective LO contains only harmonics of orders $kN \pm 1$.

There are various implementation alternatives for the elementary mixers in HRM. Current commutating passive mixers are a good choice, especially for zero-IF receivers, because of their lower 1/f noise and better linearity [2].

A conceptual diagram of a current commutating passive HRM is shown in Fig. 1. In order to avoid large voltage swings at the outputs of the transconductance amplifiers (TCA), their outputs should be connected to the ground in the time intervals, in which they are not used. This can be performed by dummy switches, but it is more rational to use the temporarily idle TCAs to create a quadrature channel and additional IF/baseband (BB) outputs (Fig. 2). Such outputs can be useful when more sophisticated techniques for improved harmonic rejection are employed as in [1].

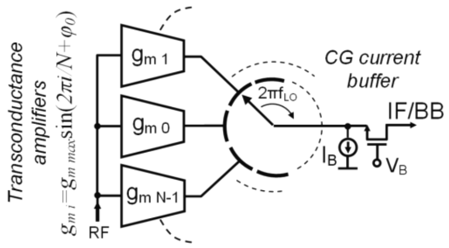

Figure 1. HRM operation principle

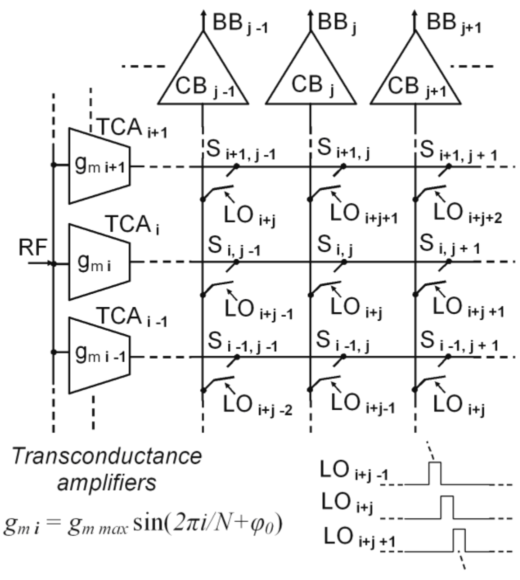

Figure 2. HRM with multiple outputs (single ended implementation).

Current buffers (CBs) can be implemented as FETs in a common gate (CG) circuit. Transimpedance amplifiers (TIA) can be used instead of CBs. The paper assumes that the input resistance of CBs (or TIAs) is much lower than switch resistance.

The discussions will be mainly focused on direct conversion receivers, as they are most affected by flicker noise.

Also, ordinary mixers will be called "simple mixers" (SM) in contrast to HRM.

In this paper we extend the SM analysis described in [3] over the HRM, which is shown in Fig. 2. The equations are derived for even N only, as the odd values are not practical. All equations apply to balanced HRM implementation.

What was found in [3] for flicker noise of CB bias sources and CB loads as well as for TCA flicker noise of SMs also applies for HRMs, which is why it will not be discussed here.

The rest of the paper is organized as follows: Sections 2 and 3 focus on flicker noise originated by the switches and by CG FETS in the CBs, respectively. Section 4 compares HRMs and SMs in terms of flicker noise level.

2. SWITCH FLICKER NOISE

The slowly varying gate-referred flicker noise of the switching FETs of the mixer randomly modulates the commutation instants. This results in a train of noise pulses which add to the ideal square-wave commutation waveforms. As a consequence, flicker noise appears at the output under certain conditions [3].

In order to examine the changes of the effective LO waveform of the HRM caused by switch flicker noise, it is appropriate to apply a DC voltage $V_{in} = 1/g_{m\max}$ to the HRM input. Then the output signal of the HRM will be numerically equal to the effective LO waveform.

Further discussion is based on the following assumptions:

1. The gate referred flicker noise voltage V_n of the FET is independent of V_{GS} [4].

2. V_n is nearly constant even within a large number of LO cycles.

3. The LO waveform transitions are linear functions of the time:

$$V_{LO} = V_{LO\min} + S\,t \text{ or } V_{LO} = V_{LO\max} - S\,t, \qquad (1)$$

where S is the slope of LO transitions.

4. FET switches are in the deep triode region, so the square-law model is accurate enough for our purposes [3]. Hence, switch conductance can be expressed as

$$g = \beta(V_G - V_B - V_{th} + V_{LO}) = \beta(V_{eff} + V_{LO}), \qquad (2)$$

where V_G and V_B are the gate and source bias voltages, respectively, V_{th} is the threshold voltage of the FETs, V_{eff} is the dc effective voltage of the switch, and $\beta = \mu C_{ox} W/L$. In the last equation μ is the channel mobility, C_{ox} is the gate oxide capacitance, and W and L are the width and the length of the switch.

We examine the commutation of the TCA$_i$ output current from the CB$_{j-1}$ input to the CB$_j$ input. The other currents have no influence, as the CB inputs act as virtual grounds. Commutation begins at time instant t_1 when $S_{i,j}$ starts to conduct and finishes at t_2 when $S_{i,j-1}$ is completely turned off (Fig. 3). Switches $S_{i,j-1}$ and $S_{i,j}$ form a current divider with current division ratios varying from 1 to 0 for the CB$_{j-1}$ input and from 0 to 1 for the CB$_j$ input linearly in the time.

Now let us consider the case when a nonzero noise voltage is present at $S_{i,j}$ gate only.

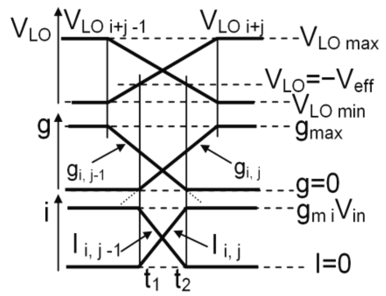

Figure 3. Commutation of TCA output from CB$_{j-1}$ input to CB$_j$ input.

The increase of gate voltage by V_n is equivalent to a time shift $\Delta = V_n/S$.

Depending on the V_n sign, this time shift increases or decreases the "on" time of the switch. As a result, modifications of the current waveforms occur. The difference between the ideal waveform and the "noisy" waveform is a pair of narrow error pulses shown in Fig. 4(a). If there is also a noise voltage at $S_{i,j-1}$ gate, the shape of error pulses changes as is shown in Fig. 4(b) or Fig. 4(c) depending on the signs of $V_{n\,i,\,j-1}$ and $V_{n\,i,\,j}$.

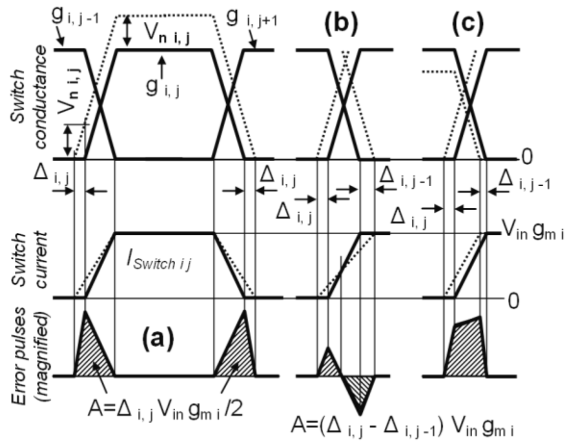

Figure 4. Error pulses at CB j input, caused by commutation of TCA i output current

Along with the commutation of TCA$_i$ current from CB$_{j-1}$ input to CB$_j$ input another commutation in progress: The TCA$_{i-1}$ current is redirected from CB$_j$ to CB$_{j+1}$. This causes a second error pulse in the CB $_j$ input. So a sum of two error pulses flows in the CB$_j$ input. It is convenient to combine these two pulses in one resultant error pulse $P_{i,\,j}$. Thus, each CB receives N different error pulses $P_{0,\,j}...P_{N-1,\,j}$ per LO cycle, spaced approximately by T_{LO}/N. According to assumption 2, the error pulse train is approximately periodic with period T_{LO}. So, the spectrum of this error pulse train contains components with frequencies $k\,f_{LO}$, where $k = 0,\,1,\,2$ etc. So, the switch flicker noise degrades the harmonic rejection ratio (HRR) of the HRM. Furthermore, the noise voltage variations in time result in changes in the LO spectrum, therefore these components are modulated by the flicker noise. In other words, switch flicker noise is up-converted to frequencies $k\,f_{LO}$. If there is a strong blocker at some of these frequencies, it will cause downconversion of the switch flicker noise to baseband.

In order to evaluate the level of the flicker noise penetrating to baseband, we will derive an expression for the mathematical expectation of squared harmonics of the error pulse train.

The harmonics of interest have numbers from 1 to $N-2$. The harmonic $N-1$ is not rejected by HRM, so blockers at $f_{Bl} \geq (N-1)f_{LO}$ are suppressed by the preselect filter of the receiver.

As the error pulses are relatively short, we replace them by time-shifted delta functions, multiplied by the area of respective error pulses. We performed Matlab simulations, which showed errors of the calculated spectra within 1.5 dB for pulse durations up to $0.25T_{LO}/N$.

After some geometrical considerations, based on Fig 4, we express the areas A_i of the pulses.

Further we express the Fourier series coefficients $C_{k,\,j}$ of the error pulse train and take the expectation of $C_{k,\,j}^2$. We assume that the flicker noise voltages $V_{\;i,j}$ are uncorrelated random variables with variances $\sigma_{i,j}^2$. The latter are inversely proportional to the FET area [2], so if the switch widths are scaled according the values of $g_{m\,i}$, then $\sigma_{i,j}^2 = \sigma_{n\min}^2 / \left|\sin(2\pi\, i/N + \varphi_0)\right|$, where $\sigma_{n\min}^2$ is the variance of the flicker noise voltage of the "unity" switch.

After doing substitutions and mathematical simplifications we obtain:

$$E\left[C_k^2\right] = 8\left(2+\cos\frac{2\pi k}{N}\right)\frac{\sigma_{n\min}^2}{T_{LO}^2 S^2}\cdot\frac{\cos(\pi/N-\varphi_0)}{\sin(\pi/N)}. \quad (3)$$

If the width of the switches is equal,

$$E\left[C_{k\,eq\,sw}^2\right] = 2N\left(2+\cos\frac{2\pi k}{N}\right)\frac{\sigma_{n\min}^2}{T_{LO}^2 S^2} \quad (4)$$

or about 1 dB lower than $E[C_k{}^2]$.

Equations (3) and (4) were verified by Matlab simulations.

Now we can find the signal to noise ratio at the HRM output as a function of the blocker power P_{bl}:

$$SNR = \frac{P_{in}}{P_{bl}}\,\frac{C_1^2}{E[C_k^2]} \approx \frac{P_{in}}{P_{bl}}\,\frac{\pi}{8N}\,\frac{T_{LO}^2 S^2}{\sigma_{n\min}^2}\left(2+\cos\frac{2\pi k}{N}\right)^{-1}. \quad (5)$$

The extent, to which the switch noise can cause a concern, is shown by an example. Let us assume that $N = 12$, $TS = 4$ and the RMS flicker noise voltage $\sigma_{n\min}$ is 100 μV. On the basis of eq. (5) we can calculate that a blocker to signal ratio of about 70 dB at the mixer input will cause 0 dB SNR at the mixer output. The HRR of the best HRMs is limited to 60-70 dB due to amplitude and phase mismatches. Therefore such a blocker will jam the desired

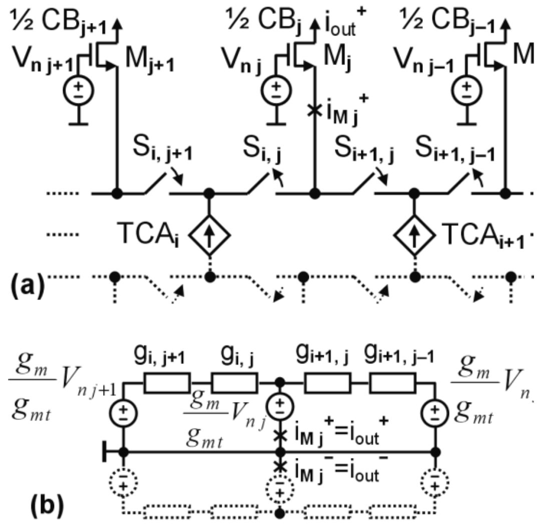

Figure 5. Commutation of CB_j from TCA_i to TCA_{i+1} (a) and corresponding equivalent circuit (b).

signal even without this noise transfer mechanism. So, the discussed mechanism can be a concern only in the best HRMs.

3. BUFFER FLICKER NOISE

The flicker noise contribution of the common gate (CG) FETs of the buffer depends on the operation of the preceding switching core [3]. Therefore, in an HRM it will be different from that in an SM, so, it will be discussed here. For their own gate referred flicker noise these FETs operate in a common source circuit. As the sources are connected to the large impedance of the bias current sources, the gain for the flicker noise should be very low. However, because the switches do not commutate instantly and there is a nonzero parasitic capacitance at the TCA outputs, the flicker noise of the CG FETs appears at the output [3]. As in [3], we will call the noise transfer mechanism which is due to imperfect commutation "direct" and that which is due to parasitic capacitance "indirect".

3.1. Buffer flicker noise, Direct

It is recommended to ensure some overlap between the "on" times of the switches [3]. As a result, during the transition time of the LO pulses, there are 4N switches in conductive state, which form low-ohmic paths between the CB inputs. Therefore, the gain of the buffer FETs for their own gate referred flicker noise will be increased. As the CB_{j-1} and CB_{j+1} inputs are virtual grounds, only 8 of these 4N switches should be taken into account for CB_j (Fig. 5). In addition, the FETs M_{j-1} and M_{j+1} act as source followers for their own gate referred noise and can be replaced by voltage sources.

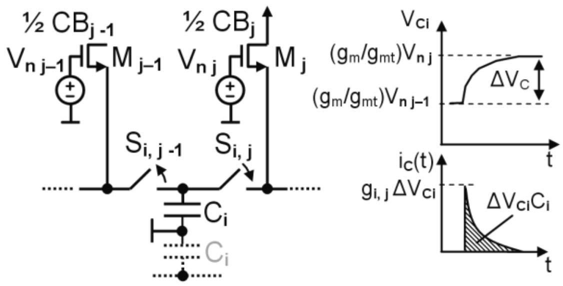

Figure 6. Arousal of noise spikes due to the indirect mechanism

The equivalent circuit is shown in Fig. 5 (b), where g_m and g_{mt} are transconductance and total transconductance (including that due to body effect) of CG FETs, respectively.

It is straightforward to express the currents i^+_{outi} and i^-_{outi} for one commutation. The differential flicker noise current in BB is equal to the difference of their time-averaged sums:

$$i_{oav} = \frac{1}{T_{LO}} \int_0^{T_{LO}} \sum_{i=0}^{N-1} i^+_{outi} dt - \frac{1}{T_{LO}} \int_0^{T_{LO}} \sum_{i=0}^{N-1} i^-_{outi} dt \, . \tag{6}$$

We take expectation of i^2_{oav}. After doing substitutions and mathematical simplifications, we obtain:

$$E\left[i^2_{oav}\right] = \frac{64}{3} \frac{\beta^2_{\max} V^4_{eff}}{S^2 T^2_{LO}} \frac{\cos^2(\pi/N - \varphi_0)}{\sin^2(\pi/N)} \frac{g^2_m}{g^2_{mt}} \sigma^2_n \approx$$
$$\approx 2.2 \beta^2_{\max} V^4_{eff} \frac{N^2}{S^2 T^2_{LO}} \frac{g^2_m}{g^2_{mt}} \sigma^2_n . \tag{7}$$

If the switches are equal, the noise power will be about 4 dB higher.

3.2. Buffer flicker noise, Indirect

Even if the switches commutate instantly, the flicker noise of the CG FETs appears at the buffer outputs due to the parasitic capacitance at the inputs of the switches (Fig. 6).

We assume that the time constants C_i/g_i are small enough to allow complete charging of the parasitic capacitances. When the switch $S_{i,j-1}$ is "on", the FET M_{j-1} act as a source follower and charges the parasitic capacitance C_i up to $V_{n\,j-1}\, g_m/g_{mt}$ through the conductance $g_{i,j-1}$ of $S_{i,j-1}$. When the switch $S_{i,j}$ turns on, the source current of M_j will charge C_i up to $V_{n\,j}\, g_m/g_{mt}$, producing a noise current spike at the CB_j output.

The corresponding charge, flowing through M_j, is $Q_i = C_i(V_{ni} - V_{ni-1}) g_m / g_{mt}$. There are N such spikes per LO cycle. The flicker noise in baseband (for the half of the circuit) is:

$$i_{o\,av} = \frac{1}{T_{LO}} \sum_{i=0}^{N-1} C_i \left(V_{n\,j} - V_{n\,j-1}\right). \tag{8}$$

If the parasitic capacitance is proportional to the g_{mi} values, then $C_i = C_{\max} \sin(2\pi i/N + \varphi_0)$.

We take expectation of $i_{o\,av}^2$. After doing mathematical simplifications, we obtain:

$$E\left[i_{o\,av}^2\right] = \frac{16 C_{\max}^2}{T_{LO}^2} \frac{\cos^2(\pi/N - \varphi_0)}{\sin^2(\pi/N)} \frac{g_m^2}{g_{mt}^2} \sigma_n^2 \approx \approx 1.6 \cdot \frac{N^2 C_{\max}^2}{T_{LO}^2} \frac{g_m^2}{g_{mt}^2} \sigma_n^2 \tag{9}$$

If C_i values are equal, the noise power will be about 4 dB higher.

Equations (7) and (9) were verified by Matlab simulations.

4. COMPARISON BETWEEN HRM AND SM AND DISCUSSION

In order to compare HRMs and SMs, we derived the necessary equations for SMs. They seem different from these in [3]. This is primarily because we take into account the noise of all involved FETs.

The equations for the switch noise and the CB direct and indirect noise in SMs are

$$E\left[C_k^{\,2}\right] = 64\sigma_n^2 / \left(T_{LO}^2 S^2\right) \tag{10}$$

$$E\left[i_{o\,av}^2\right] \approx 57\sigma_n^2 \left(g_m^2 / g_{mt}^2\right) \beta_{\max}^2 V_{eff}^4 / \left(S^2 T_{LO}^2\right) \tag{11}$$

$$E\left[i_{o\,av}^2\right] \approx 32\sigma_n^2 \left(g_m^2 / g_{mt}^2\right) C^2 / T_{LO}^2 . \tag{12}$$

Note that these equations are not obtained substituting N by 2 in eq. (3), (7) and (9). The SM is different from a degenerated HRM with $N=2$.

Furthermore, for the TCA in the SM it should be selected $g_m \approx (\pi/4)\, g_{\max}$ to ensure equal conversion gains of the both compared mixers. The other parameters of SM should be scaled accordingly.

Switch flicker noise: HRMs have lower flicker noise than SMs for N<10÷32, depending on the harmonic number.

Buffer flicker noise: For $N \geq 4$ (i.e. for all useful values of N) CB noise level in HRMs is higher than that in SMs and increases with increasing LO frequency.

It seems that CB noise can be decreased using smaller switches, but for a given large signal performance the g_{mi} values of TCAs should be scaled down accordingly, lowering the signal level. So, the SNR will be the same.

S can be increased, but it is limited by the HRM power budget at least.

Another way to reduce noise is to decrease N/T_{LO} N depends on the required harmonic rejection. Generally, the higher the frequency of the desired channel, the lower the needed value of N. If N was variable, it could be decreased with increasing received frequency, keeping the noise level unchanged. This raises the question of finding HRM architectures with a variable N.

If the width of the switches is scaled according to g_{mi} values, the noise level is about 4 dB lower than in the case of equal switches.

If N is big, dummy switches between the CBs can be used. Then the CB noise will be caused only by the noise voltage $V_{n\,j}$.

CB FETs flicker noise can be reduced using large devices. As they operate at BB frequencies, the corresponding rise of their parasitic capacitance is largely tolerable.

4. CONCLUSION

We derived equations for flicker noise in HRM and made comparison between HRM and SMs.

In general HRM have higher flicker noise than SMs. So, it is desirable to look for new HRM architectures with lower flicker noise.

References

[1] Zhiyu Ru et al., "Digitally-Enhanced Software-Defined Radio Receiver Robust to Out-of-Band Interference", *IEEE Journal of Solid-State Circuits*, vol. 44, 15 Dec. 2009, pp. 3359–3375.

[2] B. Razavi, *RF Microelectronics*, Prentice Hall PTR, 2011.

[3] S. Chehrazi, A. Mirzaei, A. A. Abidi, "Noise in Current-Commutating Passive FET Mixers", *IEEE Transactions on Circuits and Systems I: Regular Papers*, vol. 57, Feb. 2010, pp. 332–344.

[4] H. Darabi, A. A. Abidi, "Noise in RF-CMOS mixers: a simple physical model" *IEEE Journal of Solid-State Circuits*, Vol.35, Jan. 2000, pp. 15 – 25.